CrossMark
click for updates

Synthesis and structure of Zr(IV)- and Ce(IV)-based CAU-24 with 1,2,4,5-tetrakis(4-carboxyphenyl)benzene†

M. Lammert,[a] H. Reinsch,[a] C. A. Murray,[b] M. T. Wharmby,[b] H. Terraschke[a] and N. Stock*[a]

Two new MOFs denoted as M-CAU-24 (M = Zr, Ce) based on 1,2,4,5-tetrakis(4-carboxyphenyl)benzene (H_4TCPB) were obtained under mild reaction conditions within 15 min. The MOFs with composition $[M_6(\mu_3\text{-}O)_4(\mu_3\text{-}OH)_4(OH)_4(H_2O)_4(TCPB)_2]$ crystallise in the scu topology, a connectivity hitherto unreported for Zr-MOFs with tetracarboxylate linker molecules. Zr-CAU-24 exhibits UV/blue ligand-based luminescence.

Metal organic frameworks (MOFs) are a class of highly ordered crystalline and potentially porous materials formed by linking of inorganic and organic building units.[1] Their adjustability by varying metal cations and organic linker molecules leads to numerous modular structures[2] having extraordinarily high surface areas, tuneable pore sizes and functionalities, which makes them suitable candidates for applications in various fields, including gas storage and separation, sensor technology, catalysis and drug delivery.[3] Since the discovery of UiO-66 $[Zr_6O_4(OH)_4(BDC)_6]$ in 2008, the scientific interest especially in Zr-based MOFs has increased due to their unparalleled thermal and chemical stability. The cubic close packed framework of UiO-66 is built of hexanuclear $[Zr_6O_4(OH)_4]^{12+}$ clusters, which are twelve-fold linked by 1,4-benzenedicarboxylate ions (BDC^{2-}).[4] Isoreticular MOFs containing the hexanuclear $[M_6O_4(OH)_4]^{12+}$ cluster are known for a range of metal(IV) cations, including Hf^{4+}, U^{4+}, Th^{4+} and more recently Ce^{4+}.[5,6] The latter are of special interest for potential catalytic applications.[6] Moreover, numerous Zr-based MOFs containing the very same inorganic building unit have been reported in recent years, in which the hexanuclear clusters are coordinated by different numbers (n = 6, 8, 10, 12) of carboxylate groups of topologically different linker molecules.[7,8] The remaining co-ordinatively unsaturated Zr sites are often occupied by modulators *e.g.* formic acid, acetic acid, benzoic acid or hydroxide ions and water molecules,[9] which can also influence crystal size, morphology and crystallinity.[7,8] During the last five years, Zr-MOFs with tetracarboxylic acid linker molecules *e.g.* porphyrin derivatives[10] have been intensely investigated due to their multi-functionality as light-harvesting reagents, catalysts and in sensors.[11] Many topologically different frameworks with the same linker tetrakis(4-carboxyphenyl)porphyrin (H_4TCPP) and Zr_6O_8 nodes have been reported to form by varying the synthetic conditions.[9,12] Using the tetracarboxylic acid H_4TBAPy (1,3,6,8-tetrakis(*p*-benzoic acid)pyrene) the compound NU-1000 $[Zr_6(\mu_3\text{-}OH)_8(OH)_8(TBAPy)_2]$ was synthesized.[13] By extension of the porphyrin and pyrene linker molecules it was possible to obtain MOFs with specific BET surface areas up to 6650 m^2 g^{-1}.[14] An overview of reported Zr-MOFs containing tetradentate linker molecules is given in the ESI (Table S1†).[7,9,12–15]

Here, we present the synthesis and detailed characterisation of two new isostructural MOFs denoted as CAU-24 (CAU = Christian-Albrechts-University) with the formula $[Zr_6(\mu_3\text{-}O)_4(\mu_3\text{-}OH)_4(OH)_4(H_2O)_4(TCPB)_2]$ and $[Ce_6(\mu_3\text{-}O)_4(\mu_3\text{-}OH)_4(OH)_4(H_2O)_4(TCPB)_2]$, which are both constructed from $[M_6(\mu_3\text{-}O)_4(\mu_3\text{-}OH)_4]^{12+}$ clusters (M = Zr^{4+}, Ce^{4+}) and benzene-1,2,4,5-tetrayltetrabenzoate ions ($TCPB^{4-}$).

The title compounds were synthesized under similar reaction conditions starting from dissolving H_4TCPB in DMF, adding the corresponding aqueous metal solution and formic acid. Pure products exhibiting the highest crystallinity were obtained using short reaction times of 15 min under stirring and conventional heating at 100 °C. Details of the synthesis procedure are given in the ESI.† All compounds were only obtained as microcrystalline powders. PXRD patterns of as synthesized and thermally activated samples (140 °C and 10^{-2} kPa) are presented in Fig. 1. Due to the removal of guest molecules a shift in reflection positions in the PXRD pattern is observed. This change is reversible once the activated capillaries are subjected to ambient conditions (Fig. S1†).

[a]*Institut für Anorganische Chemie, Christian-Albrechts-Universität zu Kiel, Max-Eyth-Straße 2, 24118 Kiel, Germany. E-mail: stock@ac.uni-kiel.de*
[b]*Diamond Light Source Ltd, Diamond House, Harwell Science & Innovation Campus, Didcot, Oxfordshire, OX11 0DE, UK. E-mail: michael.wharmby@diamond.ac.uk*
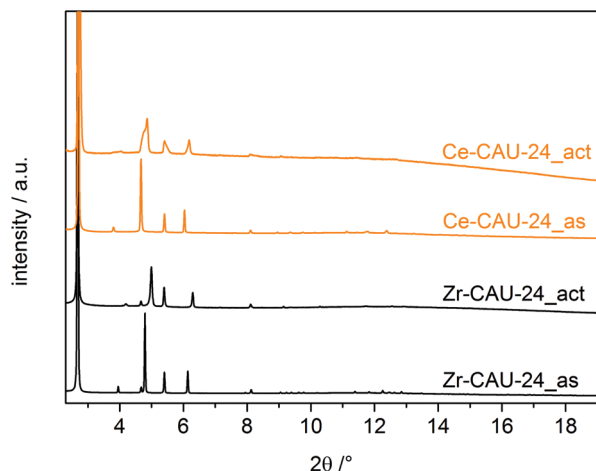
Fig. 1 Synchrotron PXRD patterns of as synthesized (as) and activated (act) Zr-CAU-24 (λ = 0.826215 Å) and Ce-CAU-24 (λ = 0.825927 Å).

A structural model was developed starting from crystal structures of Zr-MOFs that have already been reported.[9] Details are given in the ESI.† For activated Zr-CAU-24 the structural model was successfully refined using the Rietveld method and the program TOPAS[16] Academic v4.1 (Fig. S2†). Crystallographic data for the structural analysis have been deposited with the Cambridge Crystallographic Data Centre (CCDC 1490700). Tables with crystallographic parameters and selected bond lengths are reported in the ESI (Tables S2 and S3†). Due to the decreasing crystallinity of Ce-CAU-24 after activation, a Le Bail profile fit was carried out to confirm that activated Ce-CAU-24 is an isostructural analogue of the Zr-MOF (Fig. S3†). For both as synthesized products, Rietveld refinement was unsuccessful due to disordered solvent molecules inside the pores. Nevertheless, the lattice parameters were determined and phase purity was confirmed by Le Bail profile fitting in the space group *Cmmm* (Fig. S4 and S5†). After activation of both as synthesized samples (*hkl*) reflections with $l \neq 0$ are shifted to larger 2θ values which corresponds to a contraction of the unit cell along the *c*-axis (Fig. S6 and S7†). Crystallographic details for all compounds are given in the ESI (Table S4†).

In CAU-24 the $[M_6(\mu_3\text{-}O)_4(\mu_3\text{-}OH)_4]^{12+}$ clusters are organized in a C-centred orthorhombic arrangement and eight carboxylate groups are coordinated to each cluster. The other coordination sites at the Zr^{4+} ions are occupied by H_2O and OH^- molecules as described for various other Zr-MOFs. The clusters are bridged by all four carboxylate groups of $TCPB^{4-}$ linker molecules to give the formula $[M_6(\mu_3\text{-}O)_4(\mu_3\text{-}OH)_4(OH)_4(H_2O)_4(TCPB)_2]$ (M = Zr, Ce). The cavities observed are occupied by guest molecules. The clusters are connected in a **scu** topology, creating a porous framework with rhombic channels of approximately 5.3 × 10.5 Å and small pores of 2.4 × 3.5 Å in diameter (Fig. 2). Although tetradentate linker molecules have been intensely investigated, the **scu** topology has not yet been reported for Zr-MOFs.[17] A reason could be the rectangular shape of the H_4TCPB linker which can influence
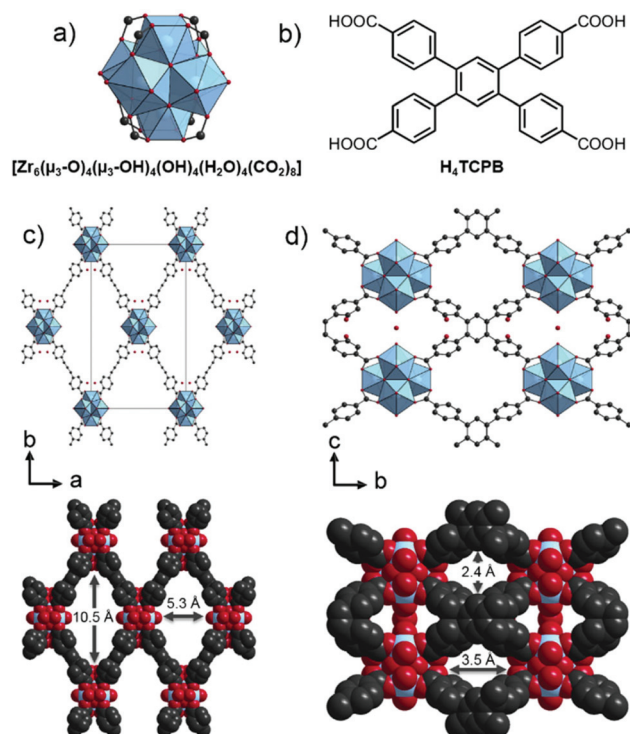

Fig. 2 Representation of the crystal structure of Zr-CAU-24. The hexanuclear $[Zr_6(\mu_3\text{-}O)_4(\mu_3\text{-}OH)_4]^{12+}$ clusters (a) are connected by $TCPB^{4-}$ linker molecules (b), here shown along [001] (c) and along [100] (d) in ball-and-stick model. The corresponding space filling models with the pore diameters obtained by taking the van der Waals radii into account are shown below, respectively.

the topology of the resulting Zr-MOF, as it was recently proposed by Matzger *et al.*[18] A representation of prominent topologies of Zr-MOFs with tetradentate linker is given in the ESI (Fig. S8†). Variable temperature powder X-ray diffraction (VT-PXRD) was carried out in quartz capillaries (0.5 mm) to investigate the thermal stability and structural changes upon thermal treatment (Fig. S9 and S14†). The as synthesized form of Zr-CAU-24 changes to the activated form at approximately 210 °C (Fig. S10†). Changes of the relative intensities and reflection positions are observed which are due to the removal of physisorbed guest molecules. These results are corroborated by thermogravimetric analysis (TGA). TGA data of as synthesized Zr-CAU-24 exhibit a first weight loss of 10.9 wt% in the temperature range 50–290 °C (Fig. S11†). A second structural change appears for Zr-CAU-24 above 290 °C. This second weight loss of 3.6 wt% (290–420 °C) is attributed to the loss of residues of strongly adsorbed solvent molecules inside the small pores, although dehydration of the $[Zr_6O_4(OH)_4]^{12+}$ clusters, as observed for the Zr-UiO-66,[19] cannot be ruled out. Eventually the framework collapses with a weight loss of 51.0 wt% (expected 53.8 wt%) upon heating above 420 °C measured by TGA and 490 °C by VT-PXRD data, respectively. The final product was identified by PXRD to be a mixture of cubic ZrO_2 (ICSD 89429) and monoclinic ZrO_2 (Baddelyite, ICSD 89426) (Fig. S12†). The difference between the

decomposition temperature obtained by TGA (420 °C measured under air flow) and VT-PXRD (490 °C measured in quartz capillary) is attributed to different measurement conditions. Most Zr-MOFs with tetradentate linkers exhibit thermal stabilities in the range 250–500 °C, generally measured by DTA under N_2 flow (see Table S1†). Compared to those, Zr-CAU-24 possesses one of the highest thermal stabilities.

In contrast, Ce-CAU-24 exhibits a lower thermal stability up to 220 °C (Fig. S13†), although it possesses the same crystal structure. This is probably caused by the high redox potential of Ce^{4+}, which also provides application in redox catalysis as recently demonstrated for Ce-UiO-66.[6] The structural change to the activated form occurs at approximately 190 °C (Fig. S14†). TGA data show a first weight loss of 28.5 wt% assigned to the loss of physisorbed guest molecules (Fig. S15†). Decomposition of the framework occurs at 220 °C with a weight loss of 36.8 wt% (expected 38.7 wt%). CeO_2 was identified to be the residue (Fig. S16†).

The IR spectra of as synthesized and activated Zr- and Ce-CAU-24 are shown in Fig. S17† and assigned in Table S5.† The vibration bands at 1653 cm^{-1} and 1606 cm^{-1} in all spectra are due to C=O stretching vibration of adsorbed or coordinated DMF molecules and formate ions, respectively. After activation of both title compounds the C=O stretching vibration of DMF decreases. Solution ^{1}H-NMR of as synthesized and activated samples corroborate the removal of DMF but also of formic acid due to activation and confirm the incorporation of the $TCPB^{4-}$ ions without modification (Fig. S18–S21†).

N_2 sorption measurements were performed to evaluate the porosity of both title compounds. Samples were activated over night at 140 °C and 10^{-2} kPa. The N_2 sorption measurements at 77 K resulted in type I(a) isotherms which are typical for microporous materials (Fig. S22†).[20] Zr-CAU-24 exhibits a specific BET surface area of 1610 m^2 g^{-1} and a micropore volume of 0.66 cm^3 g^{-1}. This value corresponds reasonably well to the solvent accessible volume calculated from the crystal structure using PLATON[21] (0.75 cm^3 g^{-1}), which uses a random probe molecule (water) with a diameter of 2.6 Å. Because of the small pore between the $TCPB^{4-}$ molecules along [011] (2.4 × 3.5 Å, Fig. 2), PLATON fills these pores when calculating the theoretical micropore volume. In sorption measurements, these pores will probably not be accessible due to the larger kinetic diameter of the nitrogen molecule of 3.64 Å.[22] The PXRD pattern collected after the N_2 sorption experiment indicates that the Zr-MOF remains intact after activation (Fig. S23†). For Ce-CAU-24 a specific BET surface area of 1185 m^2 g^{-1} and a micropore volume of 0.49 cm^3 g^{-1} was calculated from the isotherm. Thus, compared with the specific surface area of the Zr analogue and considering their molar masses, it seems likely that this relatively lower surface area results from decreasing crystallinity caused by activation (Table S6†). This phenomenon is in agreement with the PXRD pattern collected after the N_2 sorption experiment. For Ce-CAU-24, substantial peak broadening and a higher background can be observed (Fig. S23†).

Under day light radiation, Zr-CAU-24 is colourless and emits bluish light under excitation with UV radiation (365 nm, Fig. S24†), in agreement with the recorded 3D emission and excitation spectra (Fig. S25†). This behaviour is also explained by the reflection spectrum of Zr-CAU-24 (Fig. S26†), which shows a reflectance of nearly 100% over the visible spectral range, strongly decaying at wavelengths below 368 nm. The reflectance decay indicates the onset of the optical absorption edge, allowing to estimate the bandgap energy[23] of approximately 3.4 eV for Zr-CAU-24, comparable to the values previously published for the H_4TCPB linker.[24] The emission spectrum of Zr-CAU-24 (λ_{ex} = 340 nm, Fig. S27†) shows a broad emission band with a maximum at 398 nm with full width at half maximum (FWHM) of 3901 cm^{-1}, resulting in the CIE 1931[25] colour coordinates of x = 0.1666, y = 0.0105 (Fig. S28†). Likewise, the emission spectrum of the H_4TCPB linker consists of a broad band with a maximum at 404 nm (FWHM of 3319 cm^{-1}), slightly blue shifted in comparison to values reported for the trivalent carboxylic acid 1,3,5-tri(4-carboxyphenoxy)benzene.[26] The similarity in shape and position of the emission spectra of Zr-CAU-24 and the H_4TCPB linker allows us to assign the nature of the MOF emission to be ligand-based luminescence.[27] Further investigations are necessary in order to test the function of Zr-CAU-24 as sensors e.g. for hazardous molecules,[28] due to the extended porosity and therefore expected higher interaction with adsorbed guest molecules. In contrast, no luminescence was observed for Ce-CAU-24, most probably due to the overlap between the absorbed spectral range of this MOF (Fig. S26†) and the emission of the linker (Fig. S27†), causing a self-quenching effect.

In summary two new isostructural MOFs, denoted CAU-24 based on Zr and Ce were synthesized using short reaction times and mild reaction conditions. Molecular force field simulations were employed to obtain a structural model for the subsequent Rietveld refinement. Both MOFs exhibit **scu** topology which is yet unknown for reported Zr-MOFs. Zr-CAU-24 and Ce-CAU-24 are thermally stable up to 490 °C and 220 °C, respectively, proven by temperature dependent PXRD measurements. N_2 sorption experiments reveal specific surface areas of 1610 m^2 g^{-1} and 1185 m^2 g^{-1}. In contrast to Ce-CAU-24, Zr-CAU-24 emits ligand-based bluish luminescence.

Acknowledgements

Notes and references

1 O. M. Yaghi, M. O'Keeffe, N. W. Ockwig, H. K. Chae, M. Eddaoudi and J. Kim, *Nature*, 2003, **423**, 705–714; S. Kitagawa, R. Kitaura and S. Noro, *Angew. Chem., Int. Ed.*, 2004, **43**, 2334–2375; G. Férey, *Chem. Soc. Rev.*, 2008, **37**,

191–214; D. Farrusseng, *Metal-Organic Frameworks*, Wiley-VCH, Weinheim, 2011.

2 M. T. Wharmby, G. M. Pearce, J. P. S. Mowat, J. M. Griffin, S. E. Ashbrook, P. A. Wright, L.-H. Schilling, A. Lieb, N. Stock, S. Chavan, S. Bordiga, E. Garcia, G. D. Pirngruber, M. Vreeke and L. Gora, *Microporous. Mesoporous Mater.*, 2012, **157**, 3–17; R. Banerjee, A. Phan, B. Wang, C. Knobler, H. Furukawa, M. O'Keeffe and O. M. Yaghi, *Science*, 2008, **319**, 939–943.

3 J. R. Long and O. M. Yaghi, *Chem. Soc. Rev.*, 2009, **38**, 1201–1508; H. Furukawa, K. E. Cordova, M. O'Keeffe and O. M. Yaghi, *Science*, 2013, **341**, 1230444; C. V. Rodrigues, L. L. Luz, J. D. L. Dutra, S. A. Junior, O. L. Malta, C. C. Gatto, H. C. Streit, R. O. Freire, C. Wickleder and M. O. Rodrigues, *Phys. Chem. Chem. Phys.*, 2014, **16**, 14858–14866.

4 J. H. Cavka, S. Jakobsen, U. Olsbye, N. Guillou, C. Lamberti, S. Bordiga and K. P. Lillerud, *J. Am. Chem. Soc.*, 2008, **130**, 13850–13851.

5 S. Jakobsen, D. Gianolio, D. S. Wragg, M. H. Nilsen, H. Emerich, S. Bordiga, C. Lamberti, U. Olsbye, M. Tilset and K. P. Lillerud, *Phys. Rev. B: Condens. Matter*, 2012, **86**, 125429; C. Falaise, C. Volkringer, J.-F. Vigier, N. Henry, A. Beaurain and T. Loiseau, *Chem. – Eur. J.*, 2013, **19**, 5324–5331; C. Falaise, J. S. Charles, C. Volkringer and T. Loiseau, *Inorg. Chem.*, 2015, **54**, 2235–2242; A. Buragohain and S. Biswas, *CrystEngComm*, 2016, **18**, 4374–4381.

6 M. Lammert, M. T. Wharmby, S. Smolders, B. Bueken, A. Lieb, K. A. Lomachenko, D. D. Vos and N. Stock, *Chem. Commun.*, 2015, **51**, 12578–12581.

7 H. Furukawa, F. Gándara, Y.-B. Zhang, J. Jiang, W. L. Queen, M. R. Hudson and O. M. Yaghi, *J. Am. Chem. Soc.*, 2014, **136**, 4369–4381.

8 V. Bon, I. Senkovska, I. A. Baburin and S. Kaskel, *Cryst. Growth Des.*, 2013, **13**, 1231–1237; G. Wißmann, A. Schaate, S. Lilienthal, I. Bremer, A. M. Schneider and P. Behrens, *Microporous Mesoporous Mater.*, 2012, **152**, 64–70.

9 Y. Bai, Y. Dou, L.-H. Xie, W. Rutledge, J.-R. Li and H.-C. Zhou, *Chem. Soc. Rev.*, 2016, **45**, 2327–2367.

10 Z. Guo and B. Chen, *Dalton Trans.*, 2015, **44**, 14574–14583; S. Huh, S.-J. Kim and Y. Kim, *CrystEngComm*, 2016, **18**, 345–368; W.-Y. Gao, M. Chrzanowski and S. Ma, *Chem. Soc. Rev.*, 2014, **43**, 5841–5866.

11 A. Fateeva, P. A. Chater, C. P. Ireland, A. A. Tahir, Y. Z. Khimyak, P. V. Wiper, J. R. Darwent and M. J. Rosseinsky, *Angew. Chem., Int. Ed.*, 2012, **51**, 7440–7444; P. Horcajada, R. Gref, T. Baati, P. K. Allan, G. Maurin, P. Couvreur, G. Férey, R. E. Morris and C. Serre, *Chem. Rev.*, 2012, **112**, 1232–1268; L. E. Kreno, K. Leong, O. K. Farha, M. Allendorf, R. P. Van Duyne and J. T. Hupp, *Chem. Rev.*, 2012, **112**, 1105–1125; M. Yoon, R. Srirambalaji and K. Kim, *Chem. Rev.*, 2012, **112**, 1196–1231.

12 W. Morris, B. Volosskiy, S. Demir, F. Gándara, P. L. McGrier, H. Furukawa, D. Cascio, J. F. Stoddart and O. M. Yaghi, *Inorg. Chem.*, 2012, **51**, 6443–6445.

13 J. E. Mondloch, W. Bury, D. Fairen-Jimenez, S. Kwon, E. J. DeMarco, M. H. Weston, A. A. Sarjeant, S. T. Nguyen, P. C. Stair, R. Q. Snurr, O. K. Farha and J. T. Hupp, *J. Am. Chem. Soc.*, 2013, **135**, 10294–10297.

14 T. C. Wang, W. Bury, D. A. Gómez-Gualdrón, N. A. Vermeulen, J. E. Mondloch, P. Deria, K. Zhang, P. Z. Moghadam, A. A. Sarjeant, R. Q. Snurr, J. F. Stoddart, J. T. Hupp and O. K. Farha, *J. Am. Chem. Soc.*, 2015, **137**, 3585–3591.

15 S. Wang, J. Wang, W. Cheng, X. Yang, Z. Zhang, Y. Xu, H. Liu, Y. Wu and M. Fang, *Dalton Trans.*, 2015, **44**, 8049–8061; Z. Wei, Z.-Y. Gu, R. K. Arvapally, Y.-P. Chen, R. N. McDougald Jr., J. F. Ivy, A. A. Yakovenko, D. Feng, M. A. Omary and H.-C. Zhou, *J. Am. Chem. Soc.*, 2014, **136**, 8269–8276; S. B. Kalidindi, S. Nayak, M. E. Briggs, S. Jansat, A. P. Katsoulidis, G. J. Miller, J. E. Warren, D. Antypov, F. Corà, B. Slater, M. R. Prestly, C. Martí-Gastaldo and M. J. Rosseinsky, *Angew. Chem., Int. Ed.*, 2015, **54**, 221–226; O. V. Gutov, W. Bury, D. A. Gomez-Gualdron, V. Krungleviciute, D. Fairen-Jimenez, J. E. Mondloch, A. A. Sarjeant, S. S. Al-Juaid, R. Q. Snurr, J. T. Hupp, T. Yildirim and O. K. Farha, *Chem. – Eur. J.*, 2014, **20**, 12389–12393; D. Feng, H.-L. Jiang, Y.-P. Chen, Z.-Y. Gu, Z. Wei and H.-C. Zhou, *Inorg. Chem.*, 2013, **52**, 12661–12667; D. Feng, Z.-Y. Gu, J.-R. Li, H.-L. Jiang, Z. Wei and H.-C. Zhou, *Angew. Chem., Int. Ed.*, 2012, **51**, 10307–10310; D. Feng, Z.-Y. Gu, Y.-P. Chen, J. Park, Z. Wei, Y. Sun, M. Bosch, S. Yuan and H.-C. Zhou, *J. Am. Chem. Soc.*, 2014, **136**, 17714–17717; D. Feng, W.-C. Chung, Z. Wei, Z.-Y. Gu, H.-L. Jiang, Y.-P. Chen, D. J. Darensbourg and H.-C. Zhou, *J. Am. Chem. Soc.*, 2013, **135**, 17105–17110; H.-L. Jiang, D. Feng, K. Wang, Z.-Y. Gu, Z. Wei, Y.-P. Chen and H.-C. Zhou, *J. Am. Chem. Soc.*, 2013, **135**, 13934–13938; T.-F. Liu, D. Feng, Y.-P. Chen, L. Zou, M. Bosch, S. Yuan, Z. Wei, S. Fordham, K. Wang and H.-C. Zhou, *J. Am. Chem. Soc.*, 2015, **137**, 413–419; M. Zhang, Y.-P. Chen, M. Bosch, T. Gentle, K. Wang, D. Feng, Z. U. Wang and H.-C. Zhou, *Angew. Chem., Int. Ed.*, 2014, **53**, 815–818; Y. Chen, T. Hoang and S. Ma, *Inorg. Chem.*, 2012, **51**, 12600–12602; Q. Lin, X. Bu, A. Kong, C. Mao, X. Zhao, F. Bu and P. Feng, *J. Am. Chem. Soc.*, 2015, **137**, 2235–2238.

16 A. Coelho, *TOPAS-Academics, v4.1, Coelho Software*, Brisbane, Australia, 2012.

17 During the publication process a porphyrin-based MOF named NU-902 exhibiting a scu topology was reported by P. Deria, J. Yu, R. P. Balaraman, J. Mashni and S. N. White, *Chem. Commun.*, 2016, **52**, 13031–13034.

18 J. Ma, L. D. Tran and A. J. Matzger, *Cryst. Growth Des.*, 2016, **16**, 4148–4153.

19 L. Valenzano, B. Civalleri, S. Chavan, S. Bordiga, M. H. Nilsen, S. Jakobsen, K. P. Lillerud and C. Lamberti, *Chem. Mater.*, 2011, **23**, 1700–1718.

20 M. Thommes, K. Kaneko, A. V. Neimark, J. P. Olivier, F. Rodriguez-Reinoso, J. Rouquerol and S. W. Sing Kenneth, *Pure Appl. Chem.*, 2015, **87**, 1051–1069.

21 A. L. Spek, *PLATON, a Multipurpose Crystallographic Tool*, Utrecht University, Utrecht, The Netherlands, 2010.

22 C. R. Reid, I. P. O'koye and K. M. Thomas, *Langmuir*, 1998, **14**, 2415–2425.

23 M. C. Tamargo, *II-VI Semiconductor Materials and their Applications*, CRC Press, 2002, p. 125; T. Nguyena and A. R. Hind, *The Measurement of Absorption Edge and Band Gap Porperties of Novel Nanocomposite Materials*, Varian Cary 500 Spectrophotometer, Manual No. 081.

24 Z. Hu, G. Huang, W. P. Lustig, F. Wang, H. Wang, S. J. Teat, D. Banerjee, D. Zhang and J. Li, *Chem. Commun.*, 2015, **51**, 3045–3048.

25 P. R. Boyce, *Human Factors in Lighting*, CRC Press, 3rd edn, 2014.

26 H. He, F. Sun, T. Borjigin, N. Zhao and G. Zhu, *Dalton Trans.*, 2014, **43**, 3716–3721.

27 W. W. Lestari, P. Lönnecke, H. Cerqueira Streit, M. Handke, C. Wickleder and E. Hey-Hawkins, *Eur. J. Inorg. Chem.*, 2014, **2014**, 1775–1782; W. W. Lestari, P. Lönnecke, H. Cerqueira Streit, F. Schleife, C. Wickleder and E. Hey-Hawkins, *Inorg. Chim. Acta*, 2014, **421**, 392–398.

28 S. Sanda, S. Parshamoni, S. Biswas and S. Konar, *Chem. Commun.*, 2015, **51**, 6576–6579.